JPE 15-3-24

http://dx.doi.org/10.6113/JPE.2015.15.3.819
ISSN(Print): 1598-2092 / ISSN(Online): 2093-4718

Multiple-Period Repetitive Controller for Selective Harmonic Compensation with Three-Phase Shunt Active Power Filter

Chao Zhang*, Maofa Gong†, Yijun Zhang**, and Yuxia Li*

*†College of Electronic Eng. and Automation, Shandong University of Science and Technology, Qingdao, China
**Longkou Mineral Group Co. Ltd., Longkou, China

Abstract

This paper presents a shunt active power filter (SAPF) for compensating inter-harmonics and harmonics when inter-harmonics content is evident in the grid. The principle of inter-harmonics generation in the grid was analyzed, and the inter-harmonics effect on repetitive controllers was discussed in terms of control performance. Traditional repetitive controllers are not applicable in inter-harmonic compensation. Moreover, the effect of an ideal controller on harmonics signals was analyzed on the basis of the internal model principle. The repetitive controller was improved in the form of a basis function according to theoretical analysis. The finite-dimensional repetitive controller, which is also called the multiple-period repetitive controller, was designed for the control of multiple periodic signals. A selective harmonic compensation system was developed with SAPF. This system can be used to compensate harmonics and inter-harmonics in the grid. Finally, system control performance was verified by simulation and experimental results.

Key words: Inter-harmonics, Multiple-periodic repetitive controller (MPRC), Selective harmonic compensation

I. INTRODUCTION

The main harmonics and inter-harmonics sources in coal mine gridare inverters, electric arc furnaces, and other electronic equipment [1]-[3]. Nonetheless, the harmonics characteristics of the inverter and of the electric arc furnace are dissimilar [4], [5]. The measured harmonics spectrum of a fan inverter for coal mining enterprises is shown in Fig. 1.
Characterized harmonics are the main component of harmonic currents for the harmonic sources of inverters [6]-[8]. Harmonic sources do not affect the safe operation of the grid given the selective compensation of harmonics. Thus, all harmonics need not be compensated. Selective harmonic compensation increases the robustness of the control system to avoid mutual interference. Furthermore, it can reduce overall power consumption through the shunt active power filter (SAPF).

The selective harmonic compensation of SAPF is a new method of compensating harmonic currents and is a new control strategy [9], [10]. This compensation control is advantageous over the harmonics compensation mode as a whole in the following ways: first, SAPF can compensate for harmful harmonics with the limited capacity of the system when capacity exceeds the rated capacity of harmonic compensation in SAPF. Second, the system parameters vary at different frequencies; thus, selective harmonic compensations can be designed individually for different frequency harmonics to improve the robustness of the system.

At present, selective harmonic current compensation is often implemented by extracting the desired harmonics from a detection system. The harmonics are then compensated in the controller. However, the conventional proportional—integral (PI) controller induces static error. Repetitive controllers can improve compensation accuracy; however, their robustness is poor. Furthermore, disturbances easily destabilize the control system [11].

Repetitive control can track the reference signal and suppress the periodic disturbance signal. Pulse-width

Manuscript received Sep. 12, 2014; accepted Feb. 24, 2015
Recommended for publication by Associate Editor Kyo-Beum Lee.
†Corresponding Author: skdgong_ceea@163.com
*College of Electronic Eng. and Automation, Shandong University of Science and Technology, China
**Longkou Mineral Group Co. Ltd., China

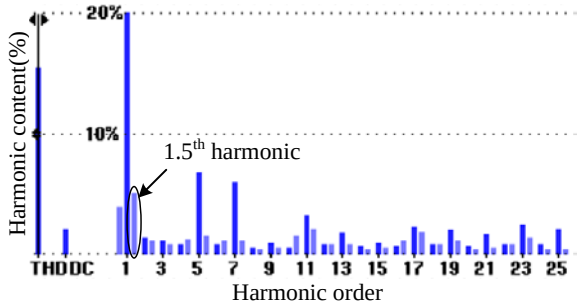

Fig. 1. Measured harmonics spectrum of a fan inverter for coal mining enterprises.

modulation (PWM) converters can be implemented to improve current control performance. However, the repetitive control system is ineffective in terms of non-periodic control and the suppression of non-period interference signals. Thus, we must improve the repetitive control system of non-period signals.

Concepts developed in this respect include the high-order repetitive controller (HORC) [12] and the adaptive repetitive controller [13]. The latter consists of two parts: a controller that can adapt to the internal signal generator period and a controller that can adjust to the sampling period. Both methods are based on adaptive control and still need a frequency observer. As a result, control system stability is difficult to analyze. HORC can also solve the conventional repetitive control problem.

Kim [14] and Inoue [15] proposed an HORC to reduce the effect of the non-periodic signal under the constraints of periodic signal control. Steinbuch [16] designed a robust repetitive controller based on convex optimization to improve the robustness of the control signal given the relative sensitivity of the error and shaping functions.

Pipeleers [17] proposed an HORC that introduces a trade-off curve through which it considers the different control commands and levels of uncertainty periodic signals. This system can then account for uncertain periods or the robustness of changed cycle signals in addition to inter-harmonics sensitivity. Although these methods improved control performance, they enhanced the complexity of the system. As a result, the system is difficult to stabilize. A multiple-period repetitive controller (MPRC) was proposed for periodic signals containing both fundamental and harmonic period signals. This controller was extended to multiple input-multiple output systems [18]-[20]. MPRC is advantageous over the conventional repetitive controller given its slight delay, fast convergence, low discrete mold order, and limited storage space, among others.

In this study, SAPF is used to compensate inter-harmonics and harmonics in situations wherein the inter-harmonics content in the grid is evident. Unlike traditional methods, the selective harmonic compensation method was designed in the current loop of the SAPF compensation controller to avoid incurring problems in the proposed detection system. The MPRC was improved on the basis of the same internal model principle to enhance the performance of the control system and to eliminate static error control on different periodic signals. The simulation and experiment results verify that the designed control system is reliable.

TABLE I
CHARACTERISTICS OF DIFFERENT FREQUENCY COMPONENTS

Terminology	Characteristic
Direct current	$k = 0$
Fundamental wave	$k = 1$
Harmonic	k is a positive integer
Inter-harmonic	$m < k < m + 1$, where $m = 0, 1, 2, \ldots$
Sub-harmonic	$0 < k < 1$

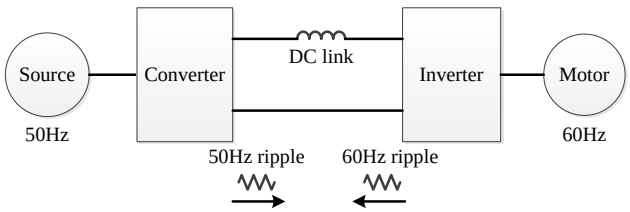

Fig. 2. Generation of inter-harmonics.

II. COMPENSATION WITH SAPF IN THE INTER-HARMONICS ENVIRONMENT

A. Inter-Harmonic Generation Principle

On the basis of the different frequency components, voltages and currents can be classified as direct, fundamental, harmonic, inter-harmonic, and sub-harmonic components. The differences among these components are presented in Table I. The component frequency is set as $f = k \times f_1$, where f_1 is the fundamental frequency (50 Hz).

The main sources of inter-harmonics are variable frequency drives, high-voltage direct currents, and other static frequency converters. The input power of these devices changes into another frequency component as the output. This system can be considered a bi-directional system because the voltages and currents at the side of the motor can be converted to the power supply side. For example, the input power frequency is 50 Hz, as shown in Fig. 2. The operating frequency of the motor is 60 Hz. This frequency is the ripple of the frequency on the DC side. Thus, the DC-side current contains both a 50 Hz ripple (from supply side) and a 60 Hz ripple (from the motor side). The current of the power supply side is connected to the DC side through the rectifier; therefore, the 60 Hz ripple manifests as the inter-harmonics of the power supply side given that 60 Hz is not an integer multiple of 50 Hz.

When a certain amount of inter-harmonics is observed in the grid, problems are encountered during SAPF operation.

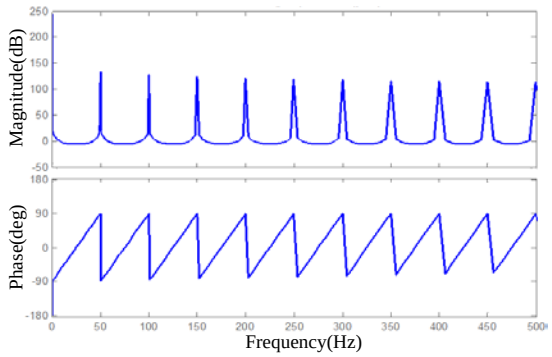

Fig. 3. Bode diagram of the repetitive controller.

The accuracy of frequency-domain methods and of reactive instantaneous power theory in inter-harmonic detection is inadequate, and test results are not completely accurate [21]. After compensation, the grid current is not as good as expected in the SAPF with repetitive controllers regardless of the adjustments made within the allowable range to the repetitive controller parameters. Harmonic compensation effect can be improved once SAPF capacity increases. However, voltage fluctuates significantly on the DC side with the large compensation current generated by the inverter.

B. Influence of Inter-harmonics on the SAPF Repetitive Control System

The accuracy of the SAPF detection system should be improved to enhance the compensation effect of the SAPF. In addition, the performance of the SAPF compensation controller must be improved. Many current repetitive controllers are used in compensation. To simplify the analysis process, a repetitive controller is given by:

$$G_{\mathrm{RE}}(z)=\frac{1}{1-z^{-N}}, \tag{1}$$

where $N = T/T_s$; T is the period of the command signal; and T_s is the sampling period. The frequency characteristic is depicted in Fig. 3.

Fig. 3 indicates that amplitude gains are infinite and that all phases are zero given the fundamental frequency and its multiples. These settings meet the integrator requirements; therefore, the static error of harmonics can be tracked. However, the frequency characteristic of the repetitive controller is not ideal for the non-integer multiples of the fundamental frequency. Thus, a satisfactory control effect cannot be exerted with only a repetitive controller under the inter-harmonic environment. This controller should be combined with other control methods to realize SAPF control.

The amplitude-frequency curve of the sensitivity function of a traditional repetitive controller was determined. The conventional repetitive controller suppresses disturbances more effectively with a fundamental frequency f = 50 Hz and with the multiple frequencies of the integer, as illustrated in

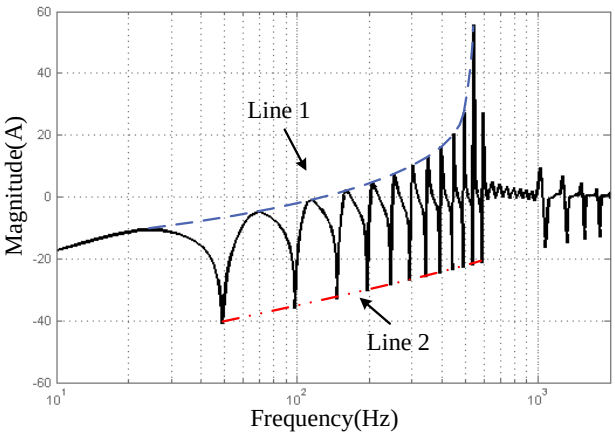

Fig. 4. Amplitude frequency of the traditional repetitive controller.

Fig. 4 line 1. However, disturbance rejection at other frequencies is worse than that in the aforementioned case. That is, the repetitive controller does not reject disturbance effectively given non-integer multiple frequencies. This finding is depicted in Fig. 4 line 2. This phenomenon can be explained by Bode integral theorem. The control performance of the system inevitably deteriorates in another band; thus, the band whose performance is declining should be disposed of in the signal band. This disposal has little effect on the system.

Therefore, inter-harmonics detection accuracy is inadequate. The capability of controllers to compensate for harmonics under the inter-harmonics environment worsens. To address this problem, finite-dimensional repetitive control is proposed to compensate the characterized harmonics and inter-harmonics of the grid and to improve the inter-harmonics compensation effect of SAPF.

III. Principle of Multiple-Period Parallel Repetitive Control And Stability Analysis

A. Principle of Multiple-period Repetitive Control

Repetitive controller design is usually applicable only for one cycle. That is, a given period of fundamental frequency and its integer multiples harmonic frequencies. However, repetitive controller performance is not ideal for traditional harmonic and inter-harmonics when the control signal contains other periodic components and given the fundamental that is part of the inter-harmonic component. When the control system contains both harmonics and inter-harmonics, these systems can be regarded as two independent control systems. Both systems can be designed separately.

The function for system transfer as a whole can be obtained by:

$$u_r(z)-d(z)=[1+R(z)G(z)]e(z), \tag{2}$$

R_1 and R_2 are the individually designed repetitive controllers for harmonics and inter-harmonics, respectively. When $Q(z) = F(z)I(z)$, the following equations are derived:

$$R_1(z) = \frac{0.95Q_1(z)C_1(z)}{z^{N_1} - Q_1(z)}, R_2(z) = \frac{0.95Q_2(z)C_2(z)}{z^{N_2} - Q_2(z)}. \quad (4)$$

Once Equation (6-21) is applied, the following can be generated:

$$u_r(z) - d(z) = \left\{ \begin{array}{l} 1 + [\frac{0.95Q_1(z)C_1(z)}{z^{N_1} - Q_1(z)} + \frac{0.95Q_2(z)C_2(z)}{z^{N_2} - Q_2(z)}]G(z) \\ + \frac{0.95Q_1(z)C_1(z)}{z^{N_1} - Q_1(z)} \frac{0.95Q_2(z)C_2(z)}{z^{N_2} - Q_2(z)} G^2(z) \end{array} \right\} e(z) . \quad (5)$$

That is,

$$[z^{N_1} - Q_1(z)][z^{N_2} - Q_2(z)][u_r(z) - d(z)] = [z^{N_1+N_2} + A + B + C]e(z) . \quad (6)$$

$$A = -[Q_2(z)z^{N_1} + Q_1(z)z^{N_2}] + Q_1(z)Q_2(z). \quad (7)$$

$$B = 0.95G(z)\{Q_2(z)C_2(z)[z^{N_1} - Q_1(z)] + Q_1(z)C_1(z)[z^{N_2} - Q_2(z)]\}$$

$$C = 0.95^2 Q_1(z)Q_2(z)C_1(z)C_2(z)G^2(z). \quad (8)$$

Sensitivity function is an important indicator of the robustness and stability of the control system. As indicated in Equation (2), this function is defined as a repetitive control transfer function between the input and error for multiple periods. That is,

$$S(z) = \frac{u_r(z) - d(z)}{e(z)} = 1 + R(z)G(z). \quad (9)$$

The repetitive controller ideal is set as in Equation (5). This ideal meets $Q(z) = 1$ and $C(z)G(z) = 1$. Let $N_1 = N_2 = N$. The following can be obtained:

$$S(z) = \frac{u_r(z) - d(z)}{e(z)} = 1 + [R_1(z) + R_2(z)]G(z) + R_1(z)R_2(z)G^2(z) . \quad (10)$$
$$= 1 + \frac{0.95(z^N - 0.05)}{(z^N - 1)^2}$$

The main principle of repetitive control is based on the error signal of the previous cycle, and the output control signal of the next cycle is obtained by the controller. The repetitive control system is defined by Equation (2). The input control signal may be superimposed on by sine waves of different frequencies, which includes the fundamental frequency and its harmonics. However, this signal also has inter-harmonic components. The MPRC can control all of the remaining cycles from the perspective of the entire band along with the high-frequency component, which is filtered out. When the control signal includes the harmonic components of various frequencies, the advantages of MPRC are enhanced. However, the control system design is complicated.

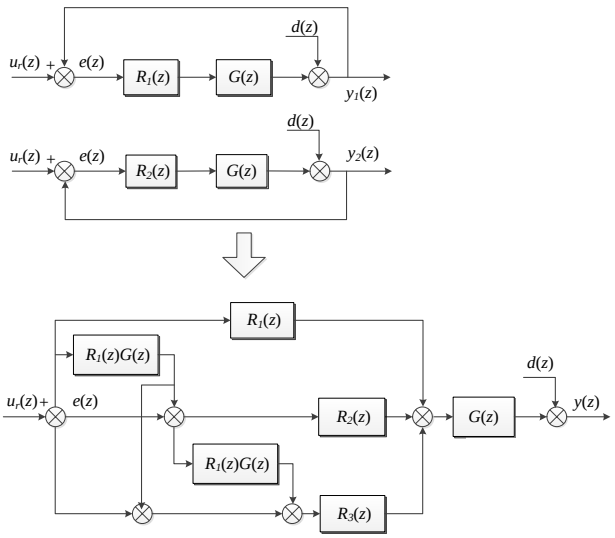

Fig. 5. MPRC system.

B. Principle of Multiple-Period Parallel Repetitive Control

Multiple-period parallel repetitive control (MPPRC) was proposed based on the concept of the basis function. A repetitive controller is individually designed for each frequency; thus, MPPRC is suitable for the limited control of harmonic component signals. The advantage of this approach is that multiple frequencies are designed in a simple controller to reduce MPRC complexity. Individual controllers can be designed for inter-harmonics, and inter-harmonic control performance can be improved.

The frequency response of the repetitive control system is input $u_r(k) = \cos(\omega kT)$, where T is the sampling time, and output $y(k) = b_n(\omega kT+\varphi)$. The input—output function can be given as the base form of the following:

$$U(k) = \frac{1}{b_n}\cos(\omega kT - \varphi). \quad (11)$$

$$Y(k) = \cos(\omega kT). \quad (12)$$

The desired signal was influenced by basis function amplitude and phase adjustment. The input basis functions in the repetitive control system can generate output basis functions. For the repetitive control system with many periodic components, the input basis function can be expressed as:

$$u(k) = \sum_{n=0}^{N} a_n U_n(k). \quad (13)$$

The corresponding output for Equation (13) can be obtained on the basis of the input basis functions that correspond to each frequency. The MPPRC system is shown in Fig. 6. Considering the entire closed-loop control system, repetitive controller $R(z)$ is defined as follows:

$$[1 + R(z)G(z)] = [1 + R_1(z)G(z)][1 + R_2(z)G(z)] = 1 + [R_1(z) + R_2(z)]G(z) + R_1(z)R_2(z)G^2(z), \quad (3)$$

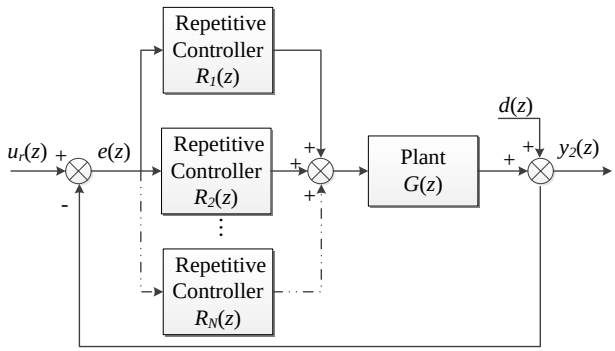

Fig. 6. MPPRC.

$$u(z) = kR(z)e(z). \quad (14)$$

$$R(z) = \sum_{n=0}^{N} k\lambda_n r_n(z). \quad (15)$$

C. Stability Criterion of Small Gain Theorem

The characteristic polynomial for the MPPRC system depicted in Fig. 6 is given as:

$$k[a_0 r_0(z) + a_1 r_1(z) + \cdots + a_N r_N(z)]G(z) = -1. \quad (16)$$

The controlled object $G(z)$ is assumed to be the stability system. Its characteristic roots are within the unit circle. Given the different basis functions $r_N(z)$, Equation (16) on the left can be combined into a common characteristic polynomial. Characteristic polynomial poles are combinations of basic function poles. When k = 0, MPPRC poles are basis function poles. When z is arbitrarily close to one pole p_N, the characteristic polynomial basis function a_N that is included in z-p_N items is close to zero. The other basis function a_M ($M \neq N$) is far from zero. In this case, the characteristic polynomial can be written as:

$$\begin{aligned} &k[a_0 r_0(z) + \cdots + a_{N-1} r_{N-1}(z)]G(z) + ka_N r_N(z)G(z) \\ &+ k[a_{N+1} r_{N+1}(z) + \cdots + a_M r_M(z)]G(z) = -1 \end{aligned}. \quad (17)$$

When k = 0, the first and the third terms of Equation (17) constitute an arbitrary function multiplied by zero. Thus, the result is zero. The conditions of Equation (17) are dictated by the middle term. Basis function a_N contains k = 0 and the denominator includes z-p_N = 0. Equation (17) can then be written as:

$$ka_N r_N(z)G(z) = -1. \quad (18)$$

The various repetitive controllers for MPPRC system are independent for each specified period. These controllers are individually designed, and their stabilities are independent of one another.

D. Sensitivity Function Analysis

The sensitivity function can reflect the performance of a repetitive control system. Thus, the sensitivity function of the MPPRC system was analyzed to verify the control performance of this system. Using Equation (16), the sensitivity function of MPPRC system was obtained as follows:

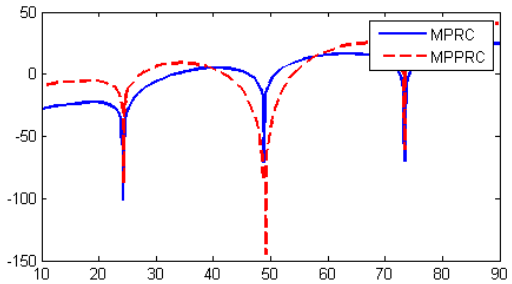

Fig. 7. Comparison of the sensitivities of MPRC and MPPRC.

$$S(z) = 1 + R(z)G(z) = 1 + k[R_1(z) + R_2(z)]G(z). \quad (19)$$

Given that $R(z)$ is the traditional repetitive controller and that the basis function satisfies Equation (11), substituting $R(z)$ into Equation (19) yields the following equation:

$$S(z) = 1 + k[\frac{0.95Q(z)C(z)}{z^{N_1} - Q(z)} + \frac{0.95Q(z)C(z)}{z^{N_2} - Q(z)}]G(z). \quad (20)$$

$Q(z)$ = 1, N_1 = 25, and N_2 = 50 are set. The amplitude-frequency characteristics of the sensitivity function of the control methods with MPRC and MPPRC can be calculated separately with Equations (6-41) and (7-10). The results are depicted in Fig. 7. The control system displays good control performances at 50 and 25 Hz.

IV. Basis Function Selection and Parameter Design

With reference to Eq. (1), the frequency domain characteristics of repetitive controller can be given as:

$$G(j\omega_k) = \frac{1}{1 - e^{-j\omega_k T}} = \frac{1}{1 - \cos\omega_k T + j\sin\omega_k T},$$

where T is the fundamental component cycle of a periodic reference signal. This signal contains the following frequency component:

$$\omega_k = \frac{2\pi k}{T} \quad k = 0,1,2,\cdots.$$

Given $G(j\omega) = \infty$, the repetitive controller experiences infinite gain at each harmonic frequency of the periodic signal.

Furthermore, the repetitive controller generates infinite poles in the imaginary axis, which are expressed as $jk\omega$, k = 0, 1, 2.... However, only a finite number of poles in the low-frequency part can affect control system performance. The infinite poles of repetitive controllers are unnecessary for steady-state performance. These poles influence the stability and transient performance of the system.

To generate the finite-dimensional repetitive controller that has the same effect as $G(s)$, $G(s)$ is written in the form of multiple poles multiplied.

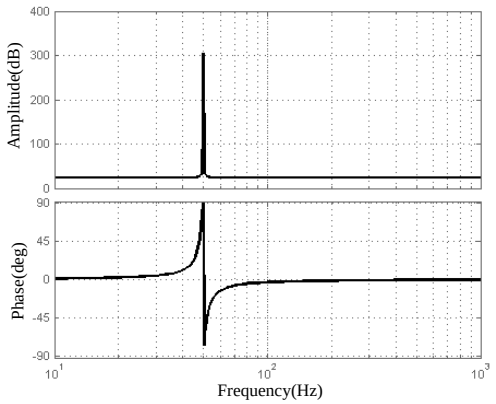

Fig. 8. Bode diagram of the basis function.

$$G(s)=\sum_{k=1}^{\infty}\frac{(s+k\omega)^2}{s^2+(k\omega)^2},$$

where $k\omega$ corresponds to the different period signals. When k is a finite integer, G(s) is a finite-dimensional repetitive controller. This variable can be used to eliminate the fundamental disturbance signal and its limited harmonics. When the power grid supplies power to inverters and other power electronic devices, 5th and 7th characteristic harmonics are mainly generated, along with 1.5th inter-harmonics. Once the characteristic harmonics of the power grid are compensated, the situation can be improved.

A. Analysis of Basis Function

The ideal controller for the signal with a resonance frequency similar to the 5th and 7th harmonics may refer to the PI controller in controlling the DC in the rotating coordinate system and realizing infinite gain for the resonant frequency signal in a two-phase stationary coordinate system. The static error of the signal is not controlled. Furthermore, phase offsets and gains are not generated at other frequencies. In general, the transfer function is given as follows:

$$r(s)=\frac{2K_i s}{s^2+\omega^2}, \tag{21}$$

where K_i is the integral coefficient and ω is the resonant frequency.

However, the frequency characteristic described above is observed only in the ideal controller. Thus, this characteristic is difficult to realize in practice. First, a resonance controller with an infinite gain is difficult to implement in an analog or a digital system. The ideal frequency characteristic of the controller is displayed in Fig. 8.

Second, reducing the gain of the basis function at other frequencies of the current cannot eliminate the harmonics effect caused by voltage. Therefore, the basis function of the transfer function is written as:

$$r(s)=\frac{2K_i\omega_c s}{s^2+2\omega_c s+\omega^2}, \tag{22}$$

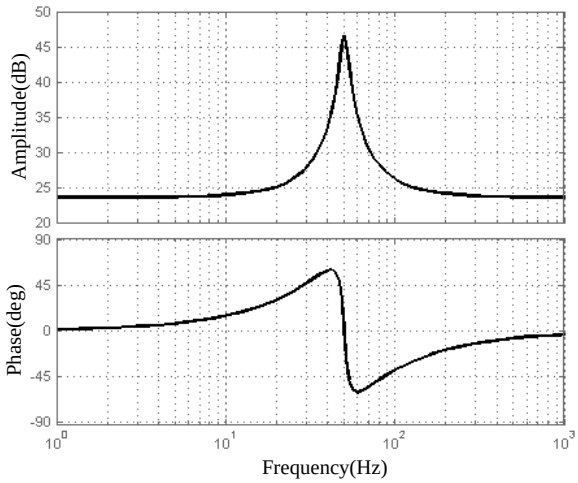

Fig. 9. Bode diagram of the basis function.

where ω_c is the cutoff frequency.

The frequency characteristic of the basis function is exhibited in Fig. 9.

In this case, controller gain is sufficiently large at the resonance frequency and a certain bandwidth is achieved. The effect generated by changes in voltage frequency can therefore be avoided.

B. Design of Basis Function Parameters

The basis function has two control parameters, namely, the integral coefficient K_i and the cutoff frequency ω_c. To determine the effect of each parameter on controller performance, one parameter remains unchanged, whereas another parameter is changed. This process is illustrated in Fig. 10.

First, ω_c = 15 is set to obtain the frequency characteristic curve with the variation of K_i. This variation is depicted in Fig. 6. K_i can influence system gain, but it does not affect system bandwidth. The gain at the resonance frequency increases when K_i increases.

K_i = 200 is then set to determine the frequency characteristic curve with the variation of ω_c. Changes in ω_c affects both system gain and phase. Specifically, gain and phase increase with the increase in ω_c; however, these factors vary only slightly at the resonance frequency.

In summary, K_i = 200 and ω_c = 15 are selected as basis function parameters.

V. Multiple-Period Parallel Repetitive Control for Selective Harmonic Compensation

The basis function is designed for the 5th harmonic, and the transfer function is expressed as:

$$r(s)=\frac{2K_i\omega_c s}{s^2+2\omega_c s+(5\omega)^2}. \tag{4}$$

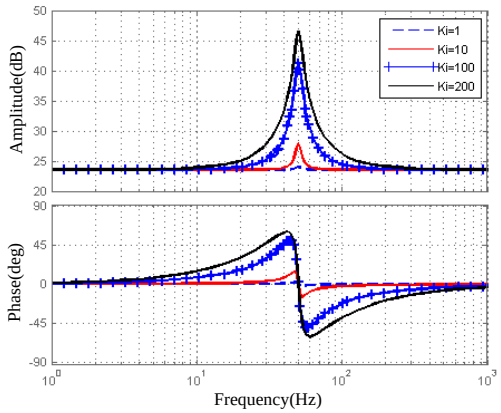

(a)

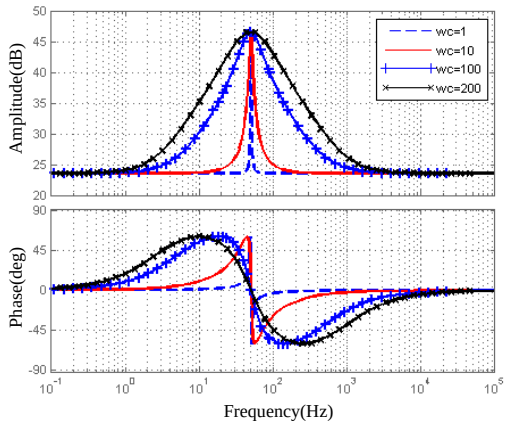

(b)

Fig. 10. Frequency responses of the basis function.

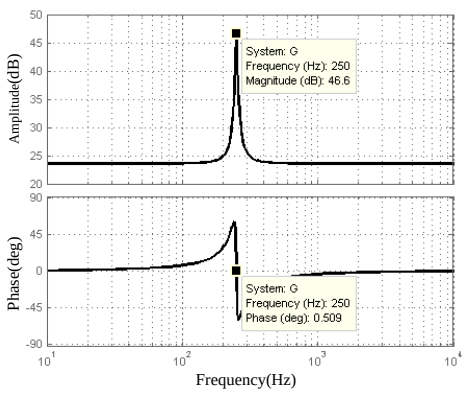

Fig. 11. Bode diagram of the basis function for the 5th harmonic.

The Bode diagram of the system is shown in Fig. 11. The controller performs well given the 5th harmonic.

The MPPRC structure is depicted in Fig. 12.

Similarly, designed basis functions are developed for the 5th, 7th, 11th, and 13th harmonics currents. The system transfer function is represented by:

$$R(s)=\sum_{n=5,7,11,13}\frac{2K_i\omega_c s}{s^2+2\omega_c s+(n\omega)^2}. \quad (5)$$

The Bode diagram of the system is illustrated in Fig. 13.

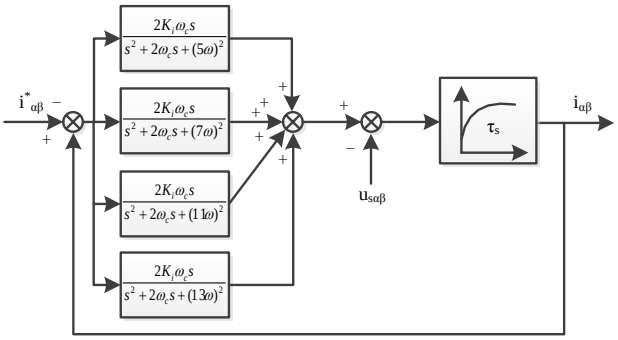

Fig. 12. MPPRC system.

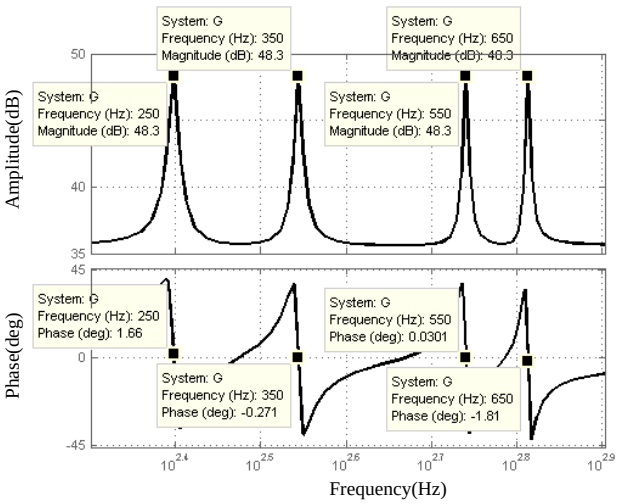

Fig. 13. Bode diagram of the basis function for harmonics.

The controller performs well for the 5th, 7th, 11th, and 13th harmonics. The basis function for the inter-harmonics is designed in consideration of the situation wherein a grid contains 1.5th inter-harmonics. The system transfer function is expressed as:

$$R(s)=\sum_{n=1.5,5,7,11,13}\frac{2K_i\omega_c s}{s^2+2\omega_c s+(n\omega)^2}. \quad (6)$$

The Bode diagram of the system is presented in Fig. 14.

The controller performs well given the 1.5th inter-harmonics. Nonetheless, a certain bandwidth must be achieved to meet the need for inter-harmonics frequency variation and to avoid the effect on the fundamental and the 2nd harmonics.

VI. Experiment Results

A. Simulation Results

Simulation experiments are presented to verify the accuracy of the method in terms of selective harmonic current control, which is based on the MPRC of the three-phase SAPF and on the situation wherein the converter is used as the harmonic source. Inverter harmonic sources normally generate 1.5th inter-harmonics. When the inter-harmonics

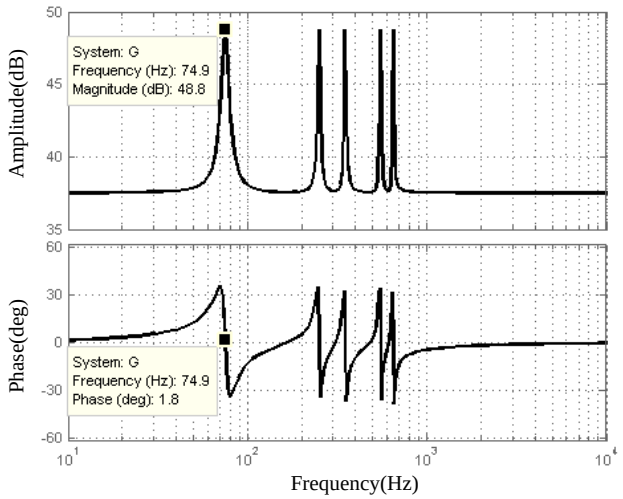

Fig. 14. Bode diagram of the basis function for inter-harmonics.

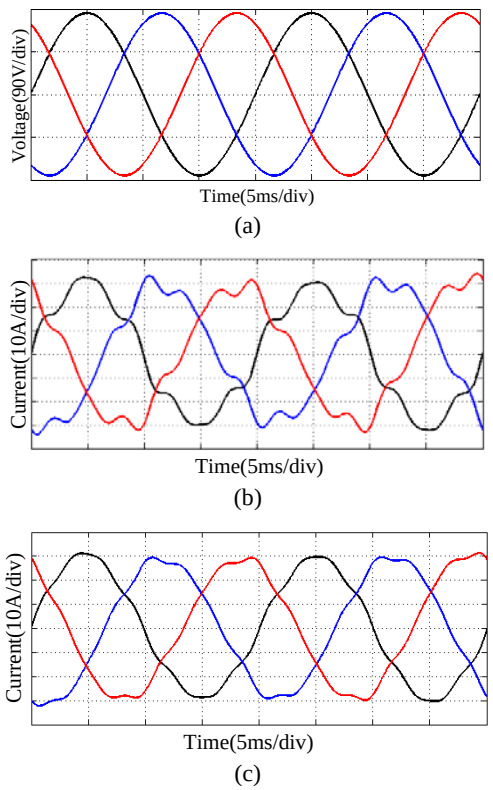

Fig. 15. Waveforms of selective harmonic compensation under the inter-harmonics environment. (a) Grid voltage waveform. (b) Grid current waveform. (c) Grid current waveform after compensation.

content is not obvious, the characteristic harmonics of the grid can be chosen for compensation. These harmonics include the 5th, 7th, and 11th harmonics. In the preceding analysis, the post-compensation current after compensation can already satisfy the requirement for safe grid operation. However, the branch of inter-harmonics compensation must increase when inter-harmonics content is evident.

Fig. 15 shows that when the grid contains inter–harmonics, MPRC is used for the 1.5th inter-harmonic and for the 5th and 7th harmonics. The current waveform of the grid after compensation is depicted in Fig. 15(c). The control of selective harmonic compensation with MPRC for harmonics currents can facilitate effective compensation.

In summary, grid currents can be compensated effectively using the MPRC-based selective harmonic compensation system whether or not these currents contain inter-harmonics. Moreover, the influence of grid voltage on the system is insignificant regardless of variation. When load mutates, the system can track the compensation signal of the grid current quickly. Therefore, this system exhibits good dynamic performance.

B. Experiment Result

The characteristics of SAPF selective harmonic compensation were verified experimentally on the three-level SAPF experimental platform. The performance of the control system was validated under different situations, such as 5th harmonic compensation and the common compensation of the 5th and 7th harmonics.

First, waveforms are presented in Fig. 16 to verify the performance of the control system under 5th harmonic compensation. Fig. 16(a) shows the waveforms of the grid current before and after compensation. The three curves from top to bottom are the DC-side voltage curve, the grid current curves before and after compensation, and the SAPF output compensation current. The scenario presented in Fig. 16(b) is generated when the curve after compensation is amplified. The DC-side voltage of SAPF stabilizes, and the distortion situation improves after compensation. To determine the compensation of the 5th harmonic, the grid current is measured before and after compensation. The grid current spectra are displayed in Figs 16(c) and 16(d). The 5th harmonic is significantly reduced after compensation; thus, the designed control system can compensate the current of this harmonic effectively.

We can compensate harmonics and inter-harmonics with different branches for the characteristic harmonic compensation of the grid using MPRC, as presented above. A compensation system was designed for the 5th and 7th harmonics to verify the performance of the control system. The generated waveform is depicted in Fig. 17. Fig. 17(a) shows the comparison of the grid current waveforms before and after compensation. The three curves from top to bottom are the DC-side voltage curve, the grid current curves, and the SAPF output compensation current. The situation depicted in Fig. 17(b) is generated when the current after compensation is amplified. The DC-side voltage stabilizes, and the distortion situation improves after compensation. The grid current is detected before and after compensation to determine the compensation effect on the 5th and 7th harmonics. Furthermore, grid current spectra are illustrated in Figs. 17(c) and 17(d). The 5th and 7th harmonics were significantly reduced after compensation; thus, the control

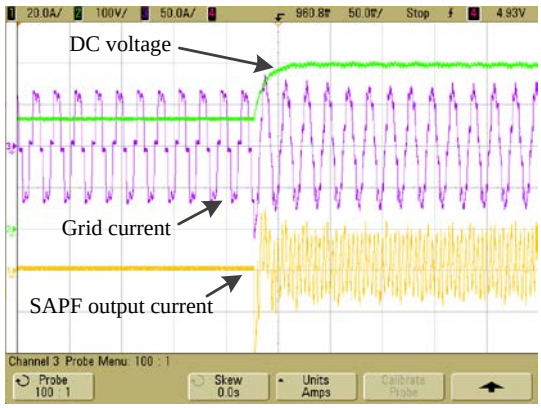

(a)

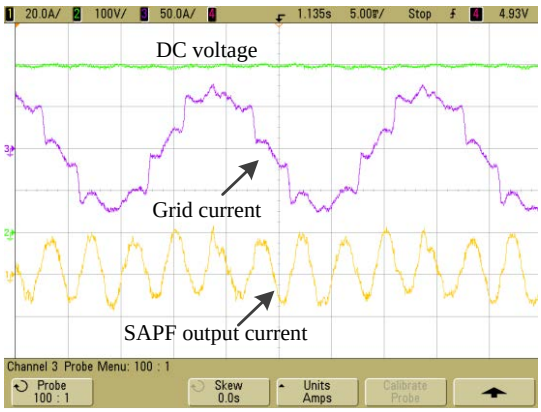

(b)

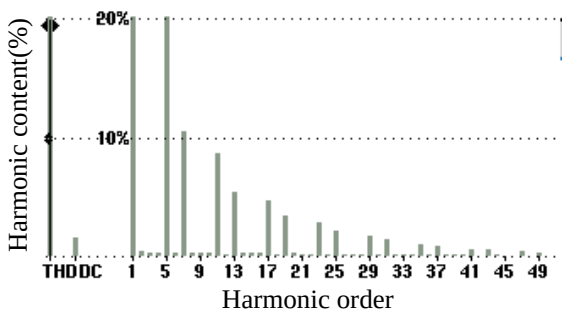

(c)

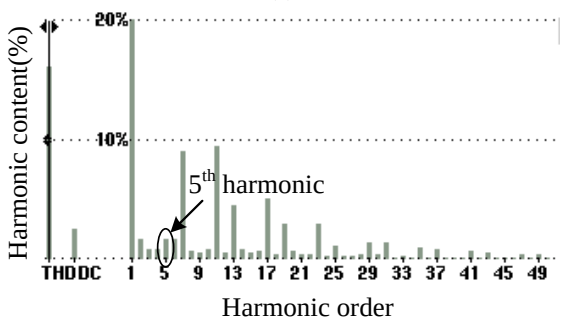

(d)

Fig. 16. Comparison of grid currents before and after compensation. (a) Grid current waveform before and after compensation. (b) Grid current waveform after compensation. (c) Grid current spectrum before compensation. (d) Grid current spectrum after compensation.

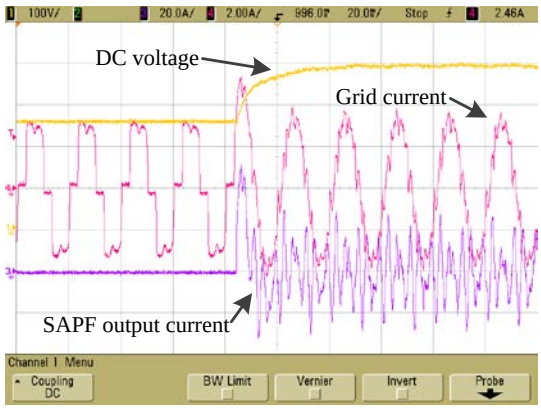

(a)

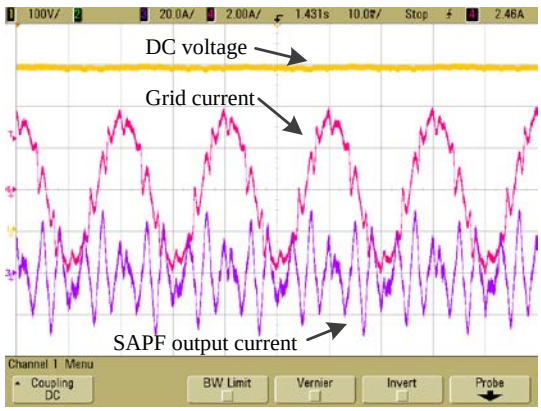

(b)

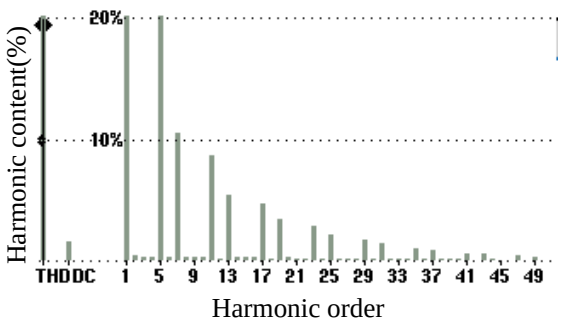

(c)

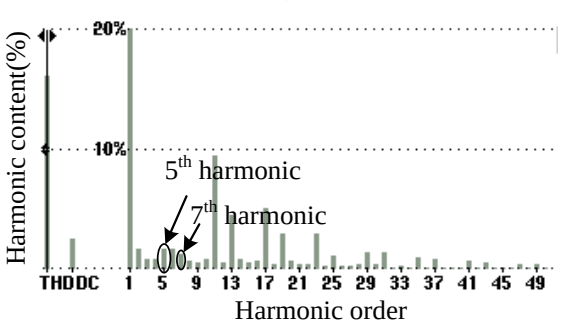

(d)

Fig. 17. Comparison of grid currents before and after compensation. (a) Grid current waveform before and after compensation. (b) Grid current waveform after compensation. (c) Grid current spectrum before compensation. (d) Grid current spectrum after compensation.

system designed for the current of these harmonics is reliable.

In summary, harmonics content was significantly reduced after compensation as a result of selective harmonic compensation control with MPRC for both single harmonic compensation and for the combination of different harmonics compensations. Therefore, the control system designed is reliable based on the experimental results. In addition, the control performance is ideal, and the compensation effect is evident.

VII. CONCLUSION

This paper presented a SAPF to compensate inter-harmonics and harmonics for situations in which the inter-harmonics content of a grid is evident. The principle of inter-harmonics generation in the grid was analyzed, and the inter-harmonics effect on repetitive controllers was discussed with respect to control performance. The traditional repetitive controller is not applicable to inter-harmonic compensation. Furthermore, the effect of an ideal controller on harmonics signals was analyzed from the perspective of the internal model principle. The repetitive controller was improved in the form of basis functions on the basis of theoretical analysis. The finite-dimensional repetitive controller, which is also called the MPRC, was designed for the control of multiple periodic signals. A selective harmonic compensation system was designed with SAPF, which can be used to compensate for the harmonics and inter-harmonics of the grid. Finally, system control performance was verified by simulation and experimental results.

ACKNOWLEDGMENT

The authors would like to thank Scientific Research Foundation of Shandong University of Science and Technology for Recruited Talents.

APPENDIX

Parameters of the three-level SAPF:

Frequency of grid voltage f = 50 Hz; line voltage e_a = 180 V; line inductance of SAPF L = 1.5 mH; DC-side capacitor C = 2200 μF; DC bus voltage U_{dc} = 360 V; sampling frequency f_k = 10 kHz; and load R_L = 8 Ω.

REFERENCES

[1] *IEEE Recommended Practice for Monitoring Electric Power Quality Industrial and Commercial Applications*, IEEE Std. 1159-2009, 2009.

[2] D. Zhang and W. Xu, "Study on the phase sequence characteristics of interharmonics," in *Proc. the CSEE*, Vol. 25, No. 12, pp. 29-34, Jun. 2005.

[3] D. Basic, "Input current interharmonics of variable-speed drives due to motor current imbalance," *IEEE Trans. Power Del.*, Vol. 25, No. 4, pp. 2797-2806, Oct. 2010.

[4] J. Yong, "Research on thyristor conduction angle characteristics in transient process of TCSC," in *Proc. the CSEE*, Vol. 28, No. 31, pp. 88-93, Nov. 2008.

[5] W. Zhao, A. Luo, H.-B. Pan, and X. Deng, "Influence of non-integer harmonics on HAPF and resolution," in *Proc. the CSEE*, Vol. 28, No. 12, pp. 73-78, Apr. 2008.

[6] N.-C. Park, H.-S. Mok, and S.-H. Kim, "Reduction of input current harmonics for three phase PWM converter systems under a distorted utility voltage," *Journal of Power Electronics*, Vol. 10, No. 4, pp. 428-433, Jul. 2010.

[7] E. K. Almaita and J. A. Asumadu, "Radial basis function neural networks (RBFNN) and p-q power theory based harmonic identification in converter waveforms," *Journal of Power Electronics*, Vol. 11, No. 6, pp. 922-930, Nov. 2011.

[8] S. Mikkili and A. K. Panda, "Real-time implementation of shunt active filter P-Q control strategy for mitigation of harmonics with different fuzzy M.F.s," *Journal of Power Electronics*, Vol. 12, No. 5, pp. 821-829, Sep. 2012.

[9] J. Miret, M. Castilla, J. Matas, J. M. Guerrero, and J. C. Vasquez, "Selective harmonic-compensation control for single-phase active power filter with high harmonic rejection," *IEEE Trans. Ind. Electron.*, Vol. 56, No. 8, pp. 3117-3127, Aug. 2009.

[10] C. Lasc, L. Asiminoaei, I. Boldea, and F. Blaabjerg, "High performance current controller for selective harmonic compensation in active power filters," *IEEE Trans. Power Electron.*, Vol. 22, No. 5, pp. 1826-1835, 2007.

[11] W. S. Chang, I. H. Such, and T. W. Kim, "Analysis and design of two types of digital repetitive control systems," *Automatic*, Vol. 31, No. 5, pp. 741-746, May 1995.

[12] T. Y. Doh and J. R. Ryoo, "Robust approach to repetitive controller design for uncertain feedback control systems," *IET Control Theory and Applications*, Vol. 7, No. 3, pp. 431-439, Feb. 2013.

[13] G. A. Ramos, J. M. Olm, and R. Costa-Castello, "Adaptive compensation strategy for the tracking/rejection of signals with time-varying frequency in digital repetitive control systems," *Journal of Process Control*, Vol. 20, No. 4, pp. 551-558, Apr. 2007.

[14] B.-S. Kim, J. Li, and T.-C. Tsao, "Two- parameter robust repetitive control with application to a novel dual-stage actuator for noncircular machining," *IEEE/ASME Trans. Mechatronics*, Vol. 9, No. 4, pp. 644-652, Dec. 2004.

[15] T. K. S. M. T. Inoue, M. Nakano, T. Kubo, S. Matsumoto, and H. Baba, "High accuracy control of a proton synchrotron magnet power supply," in *Proc. the 8th World Congress of IFAC*, Vol. 20, pp. 216-221, 2011.

[16] M. Steinbuch, S. Weiland, and T. Singh, "Design of noise and period-time robust high-order repetitive control, with application to optical storage," *Automatica*, Vol. 43, No. 12, pp. 2086-2095, Dec. 2007.

[17] G. Pipeleers, B. Demeulenaere, J. De Schutter, and J. Swevers, "Robust high-order repetitive control: Optimal performance trade-offs," *Automatica*, Vol. 40, No. 10, pp. 2628-2634, Oct. 2008.

[18] N. O. Pérez-Arancibia, T.-C. Tsao, and J. S. Gibson, "A new method for synthesizing multiple-period adaptive–repetitive controllers and its application to the control of hard disk drives," *Automatica*, Vol. 46, No. 7, pp. 1186-1195, 2010.

[19] K. Yamada, N. Li, M. Kobayashi, and H. Takenaga, "A design method for simple multi-period repetitive controllers for time-delay plants," *International Journal of Innovative Computing, Information and Control*, Vol. 5, No. 10, pp. 3313-3328, 2009.

[20] D. H. Owens, L. Li, and S. P. Banks, "Multi-periodic nonlinear repetitive control: Feedback stability analysis," *Nonlinear and Adaptive Control*, Vol. 77, No. 5, pp. 504-515, 2004.
[21] L. Zhou, M. Wu, and J. She, "Robust repetitive control design of periodically time-varying plants," *Control and Decision*, Vol. 28, No. 1, pp. 61-66, Jan. 2013.

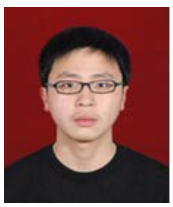

Chao Zhang was born in Zou Cheng, Shangdong, China in 1987. He received his B.S. and M.S. in 2008 and 2011, respectively, from the Shangdong University of Science and Technology, China. He received his Ph.D. in 2014 from the Department of Information and Electrical Engineering, China University of Mining and Technology. Since 2015, he has been a lecturer in the Colg. of Electronic Eng. and Automation, Shandong University of Science and Technology. His current research interests include intelligent control, power quality, and high power converters.

Maofa Gong was born in 1959. At present, he is a professor of Information and Electrical Engineering at Shandong University of Science and Technology. He is the head of the Department of Electrical Engineering and the director of the Electrical Engineering Institute. His research interests include power systems and automation, power electronics and drives, electrical theory, and new technology.

Yijun Zhang was born in Tai An, Shangdong, China in 1961. He received his B.E. degree from the Shangdong University of Science and Technology, China. At present, he works at Longkou Mineral Group Co. Ltd. He is mainly involved in coal power system security and management.

Yuxia Li is a professor at Shandong University of Science and Technology. She is the current dean of the Information and Electrical Engineering College. She is also the director of the Key Laboratory of Robotics and Intelligent Technology in Shandong Province. Her research interests include control theory and control engineering, robotics and intelligent technology, and systems engineering.